Supporting Information

Molybdenum Disulfide-Enabled Activated Carbon: a Multifunctional Adsorbent for Practical Water Treatment Applications

Environmental Science: Nano

Kfir Shapira[1], Ines Zucker[1,2*]

[1] School of Mechanical Engineering, Faculty of Engineering, Tel Aviv University, Tel Aviv 69978, Israel

[2] Porter School of Earth and Environmental Studies, Faculty of Exact Sciences, Tel Aviv University, Tel Aviv 69978, Israel

* Corresponding author; Address: Tel Aviv University, Tel Aviv 69978, Israel; Tel: (+972) 73-3804581; email: ineszucker@tauex.tau.ac.il

Contains 9 Figures, 3 Tables, 5 equations and 1 text.

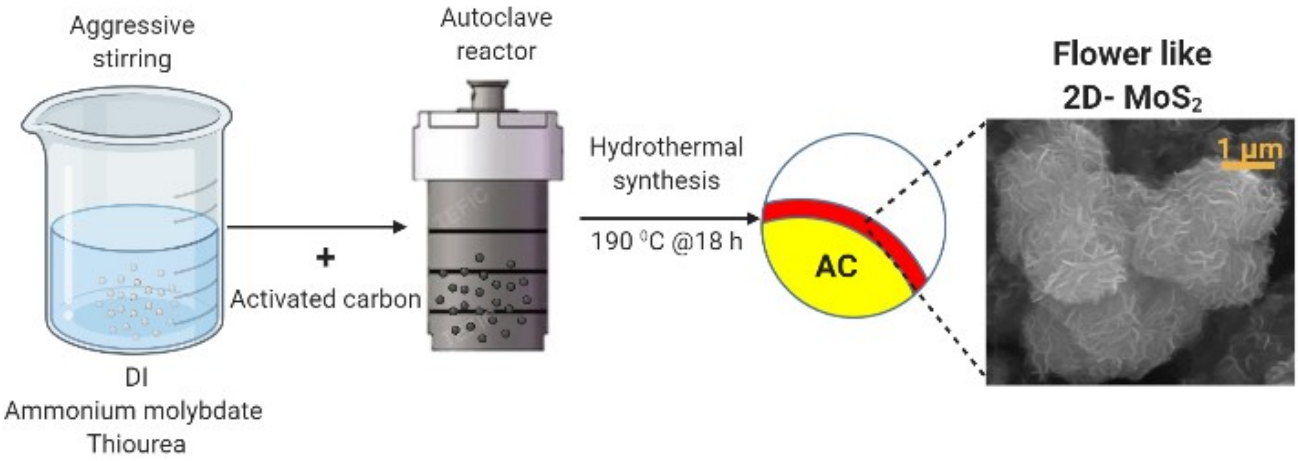

Figure S1. Schematic illustrating the molybdenum disulfide-enabled activated carbon (MoS_2@AC) synthesis procedure.

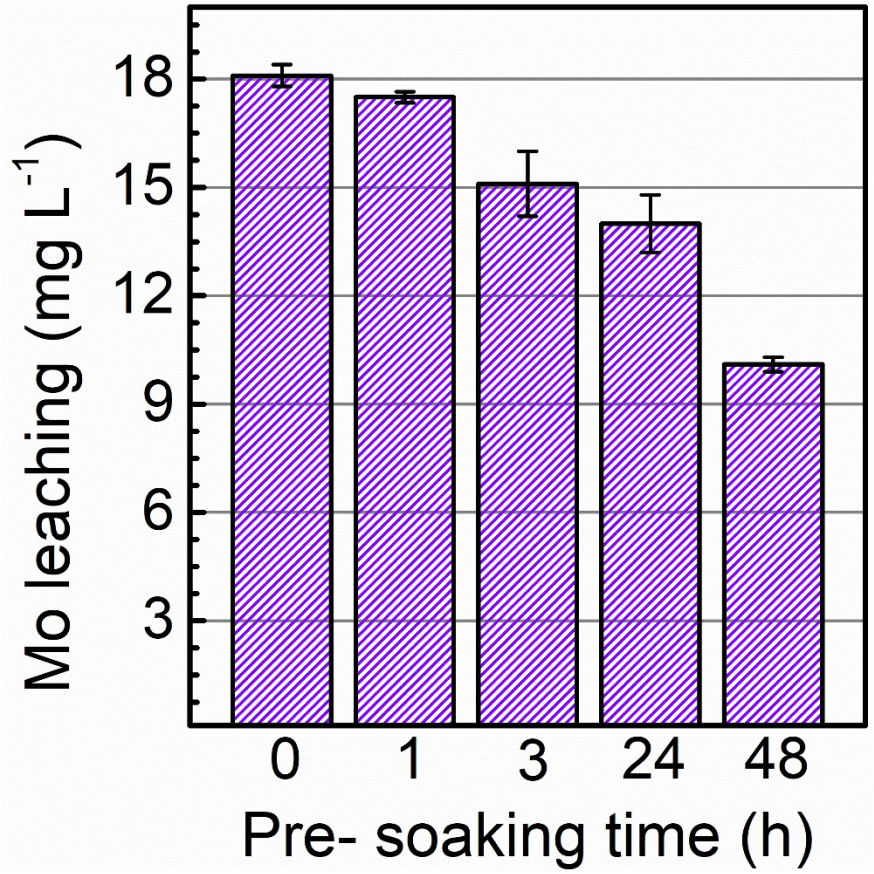

Figure S2. Molybdenum leaching following pre-soaking of the molybdenum disulfide-enabled activated carbon (MoS_2@AC) in 25 mM acetate buffer at different times. The chosen pre-soaking time was 24 hours.

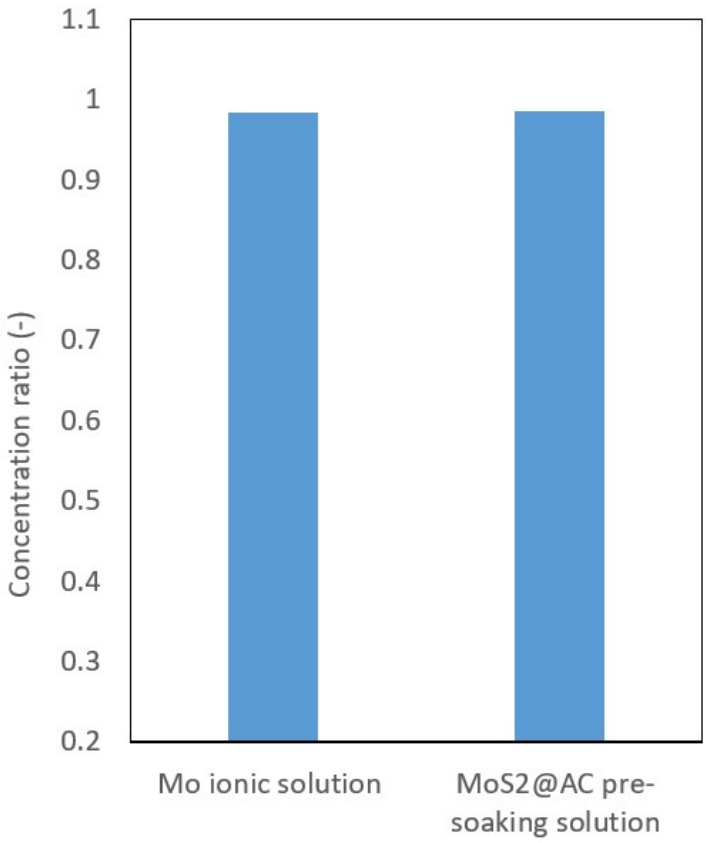

Figure S3. Investigation of the leached Molybdenum species following pre-soaking of the molybdenum disulfide-enabled activated carbon (MoS_2@AC) in 25 mM acetate buffer for 24 hours. Mo concentration in the pre-soaking solution was quantified prior to and following filtration through a 0.22 µm PVDF filter (results are shown as concentration ratio). Control experiment suggest that the filter had minor effect on the Mo concentration (left bar). As filtration did not affect the Mo concentration in the pre-soaking solution, we suggest that the pre-soaking stage mostly result in leaching of loosely-bound *dissolved* Mo compounds from the synthesized MoS_2@AC. The *dissolved* Mo species are probably composed of adsorbed precursors from the hydrothermal synthesis stage rather than the leaching of the reactive material itself.

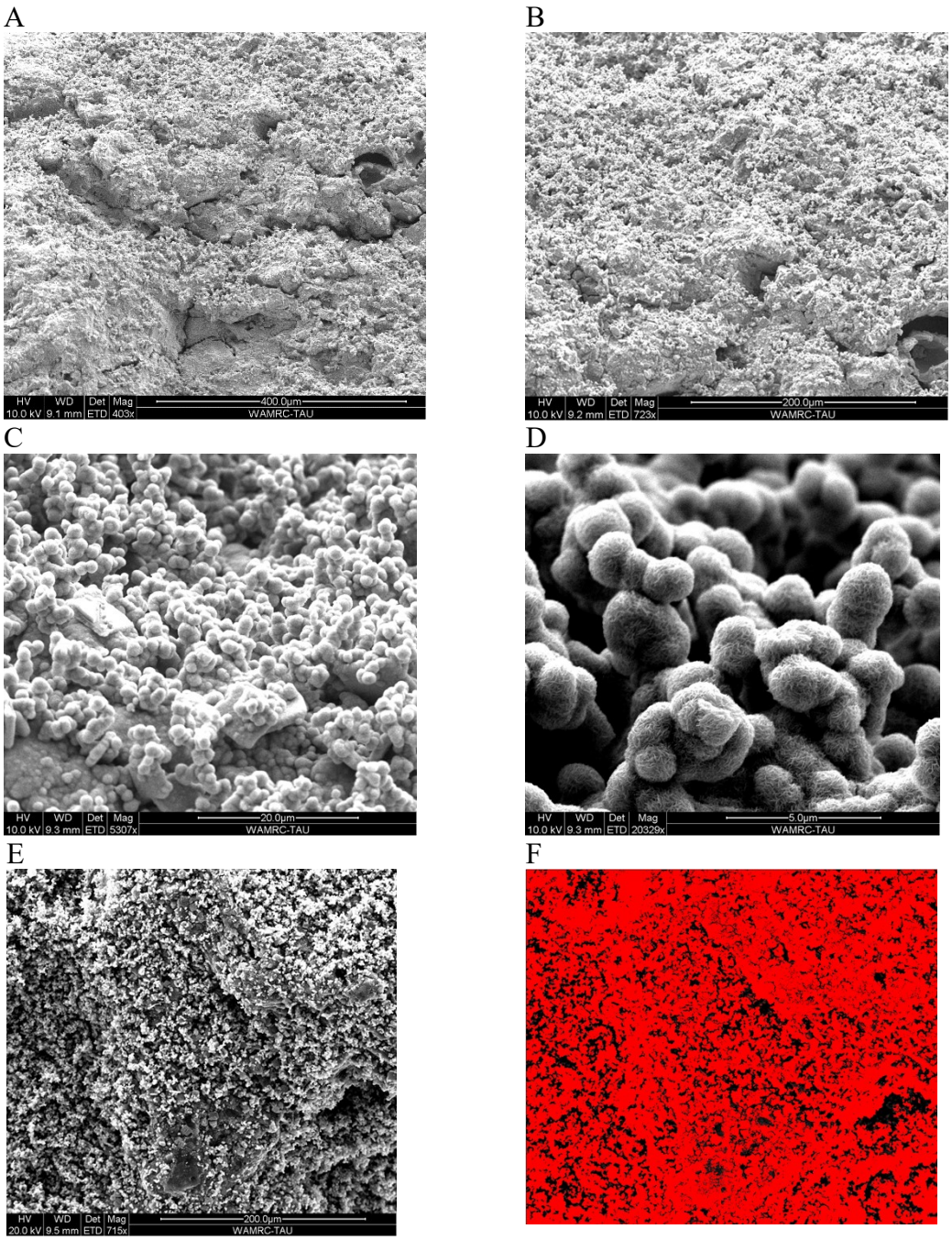

Figure S4. Scanning electron microscopy (SEM) images used for material surface analysis. (A-E) SEM images of molybdenum disulfide-enabled activated carbon (MoS_2@AC). (F) A representative analysis by ImageJ for image (E), showing the MoS_2 coverage (in red) on the AC particles.

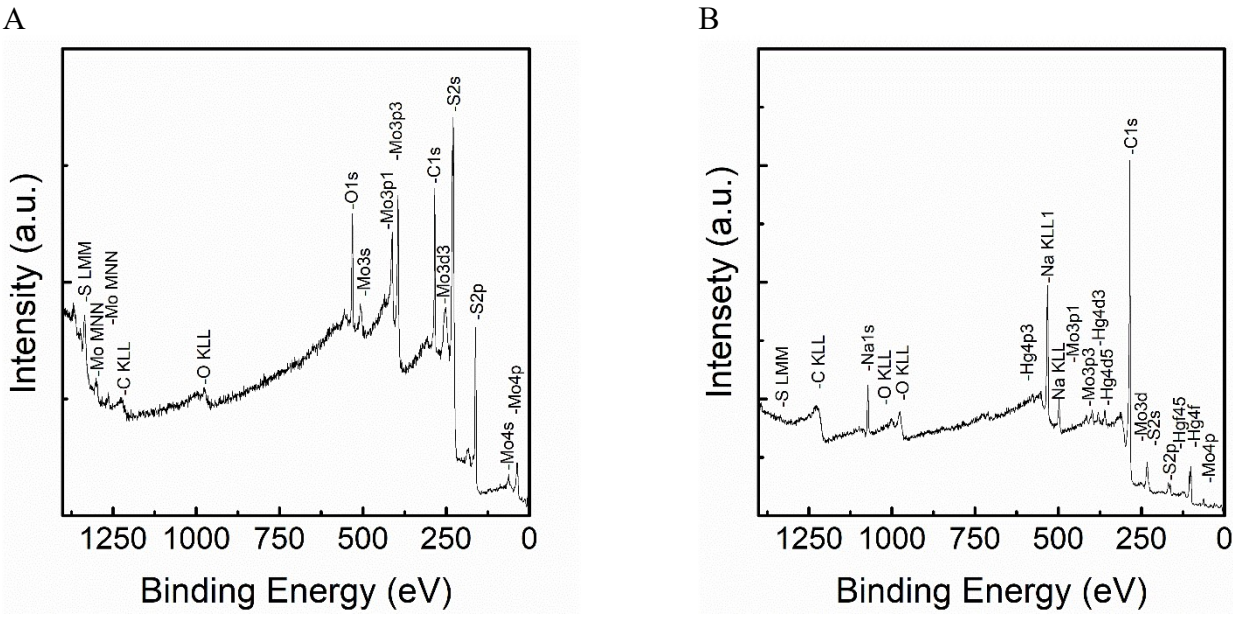

Figure S5. X-ray photoelectron spectroscopy (XPS) surveys of molybdenum disulfide-enabled activated carbon (MoS_2@AC) before (A) and after (B) mercury adsorption.

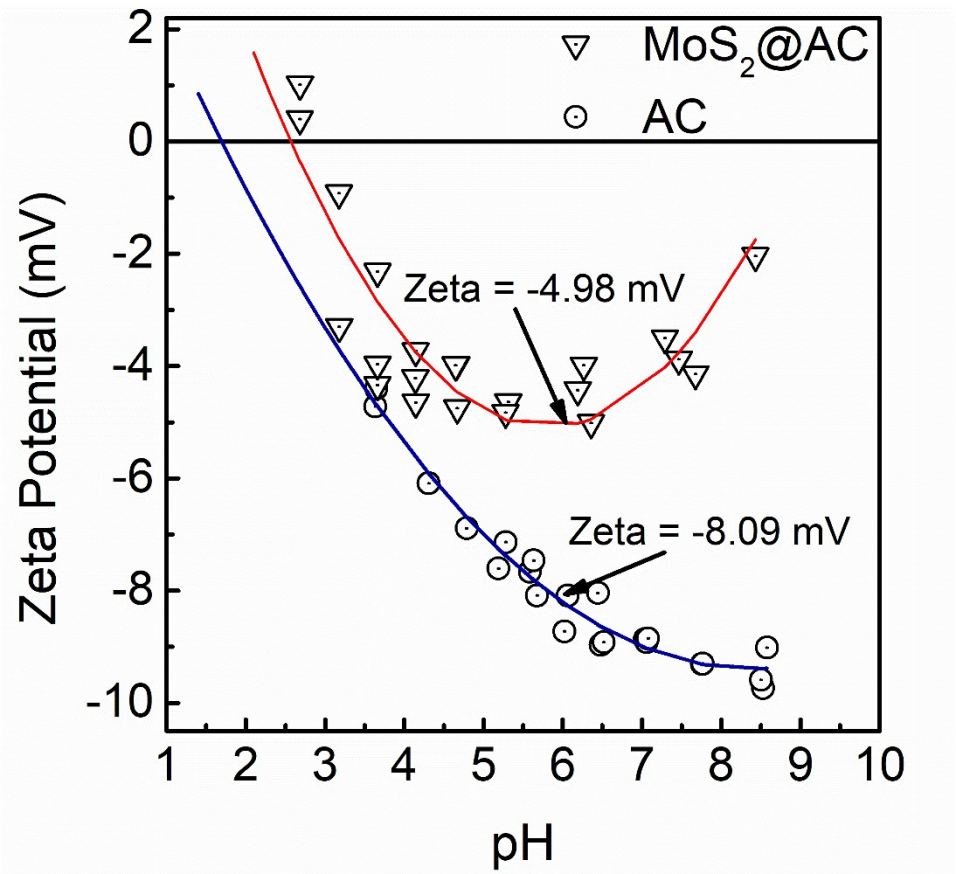

$$AC-fit$$

$$Zeta = 0.2112 \times x^2 - 3.53267 \times x + 5.3818$$

$$R^2 = 0.96052$$

$$MoS_2 @ AC - fit$$

$$Zeta = 0.485 \times x^2 - 5.639 \times x + 11.279$$

$$R^2 = 0.746$$

Figure S6. Streaming potential analysis of commercial activated carbon -Norit® 12-40 (AC), and molybdenum disulfide-enabled activated carbon (MoS_2@AC) as a function of solution pH. Fitting equations are presented as well.

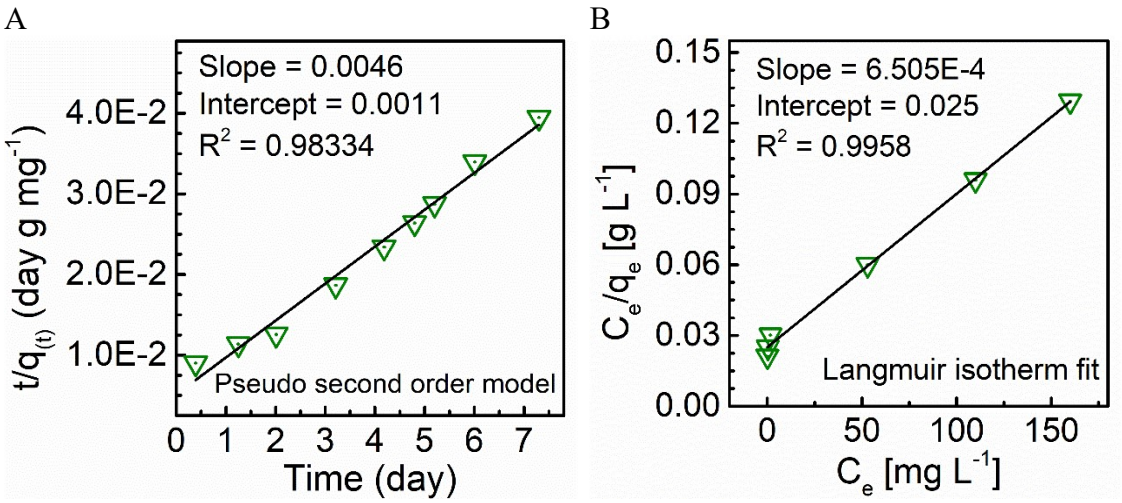

Figure S7. Kinetics and isotherm models for mercury adsorption by molybdenum disulfide-enabled activated carbon (MoS_2@AC). (A) Linear pseudo second order kinetic model fitting and (B) linear curve of Langmuir isotherm fitting.

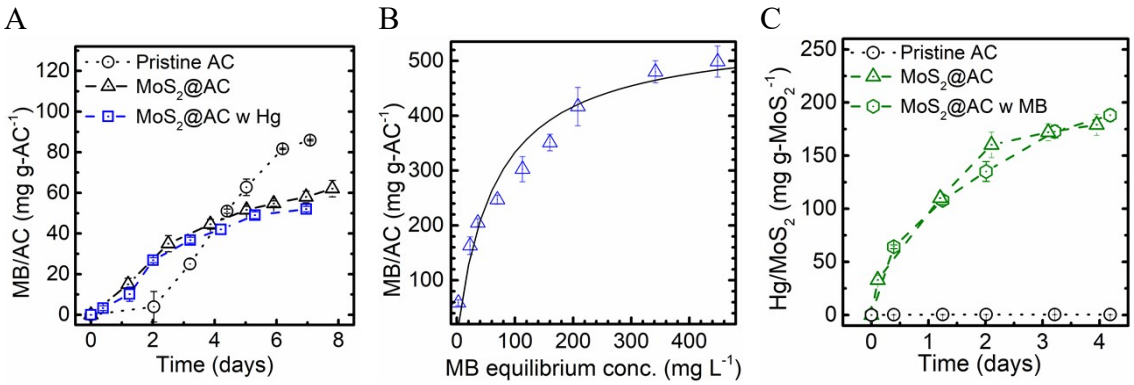

Figure S8. MoS_2@AC adsorption potential towards methylene blue and mercury as model compounds for heavy metals and organic contaminants, respectively. (A) Kinetics of removal of 10 mg L^{-1} of MB by pristine AC and MoS_2@AC in absence and presence of mercury. (B) Adsorption isotherm of MB and Langmuir fit. (C) Kinetics of removal of 10 mg L^{-1} of mercury by pristine AC and MoS_2@AC in absence and presence of MB. The removal rate in all figures is presented as a mass ratio of adsorbed pollutant to adsorbing material (i.e., MoS_2 for mercury, AC for MB).

A

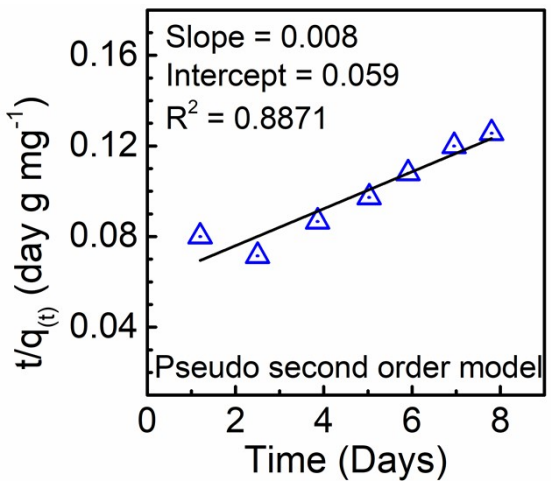

B

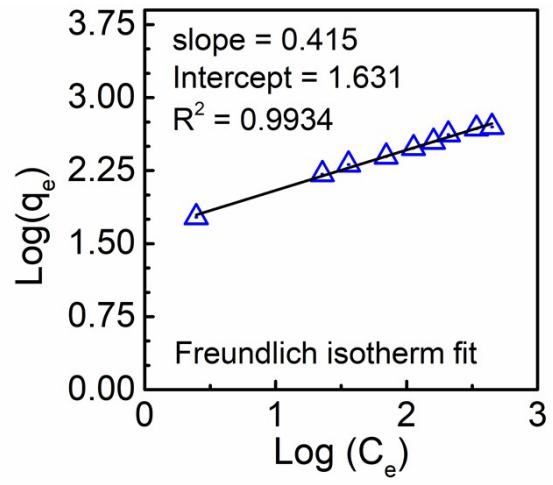

Figure S9. Methylene blue isotherm and kinetic model fitting. (A) Linear pseudo second order kinetic model fitting and (B) linear curve of Freundlich isotherm fitting.

Table S1. Groundwater characteristics used in this study, including their limit of detection (LOD).

Test	Well Depth		16.7 m
	Units	LOD	Measurement
pH			7.4
Dissolved Sodium	mg/L	0.1	4,658.00
Dissolved Calcium	mg/L	0.2	281.40
Dissolved Magnesium	mg/L	0.1	183.60
Bromide	mg/L	0.05	8.40
Fluoride	mg/L	0.3	4.10
Sulphate as SO_4^{2-}	mg/L	0.5	3,977.60
Chloride	mg/L	0.3	6,244.70
Nitrate as NO_3^-	mg/L	0.2	15.00
Nitrite as NO_2^-	mg/L	0.02	0.09
Total Organic Carbon	mg/L	2	12.00

Table S2. Kinetics and isotherm models values for mercury and methylene blue (MB). Selected models are marked in orange.

		Hg^{2+}	MB
a. First order model			
k_1	[L/day]	1.112	0.4656
q_e	[mg/g]	0.385	0.2887
R^2	-	0.856	0.8742
b. Second order model			
k_2	[g/mg/day]	0.021	0.00108
q_e	[mg/g]	217.4	125
R^2	-	0.9833	0.8871
c. Langmuir isotherm			
q_{max}	[mg/g]	1538	555.5
k_L	[L/mg]	0.025	0.0152
R^2	-	0.9958	0.9728
d. Freundlich isotherm			
k_f	$[(mg/g)*(L/mg)^{1/n}]$	39.90	42.7562
n	-	0.7165	0.415
R^2	-	0.9798	0.9934

Table S3. Simultaneous organic-inorganic removal potential by materials previously suggested in literature.

Material	Removal capacity		Reference
	Inorganic	Organic	
MoS_2@AC	Mercury 1,280 mg/g MoS_2	Methylene blue 555 mg/g AC	(this paper)
Porous organic polymer with thiol or thioether groups (POP-Sh/ POP-SMe)	Mercury 180 mg/g	Toluene and m-xylene 350-450 mg/g	(1)
TiO_2@AC/ TiO_2@CE (carbonized epoxy)	Lead 97%	Methylene blue ~90%	(2)
Betaine modified montmorillonite	Cadmium ~40 mg/g	Bisphenol A 80 mg/g	(3)
Block-co-polymer inorganic–organic hybrid material	Lead 131.6 mg/g	Phenol 18.18 mg/g	(4)

Equations used in the study. Kinetic equations were used as pseudo-first and -second order models (S1 and S2, respectively). The isotherm models used are Langmuir and Freundlich, as described in equations S3 and S4 (respectively). Adsorption capacities are $q_{(t)}$ and q_e (mg g^{-1}) at particular time points and at equilibrium, respectively. Pseudo first- and second-order rate constant are k_1 (day^{-1}) and k_2 (g mg^{-1} day^{-1}) and t represents single time point (day). The maximum adsorption capacity is q_{max} (mg g^{-1}) assessed through isotherm fit. The Langmuir and Freundlich constants are k_L (L mg^{-1}) and k_f ((mg/g)*$(L/mg)^{1/n}$), respectively. C_e is the pollution concentration (mg L^{-1}). Equation S5 is Bragg's law, where d (nm) is the interplanar spacing, θ (°) is the incidence angle, n is the diffraction order, and λ (nm) is the radiation wavelength.

Equation number	Equation	Model name	Reference
(S1)	Nonlinear: $q_{(t)} = q_e * (1 - exp(-k_1 * t))$ Linear: $log\,(q_e - q_{(t)}) = log\,(q_e) - \frac{k_1 * t}{2.303}$	Pseudo first order kinetics	(5)
(S2)	Nonlinear: $q_{(t)} = \frac{q_e^2 * k_2 * t}{1 + q_e * k_2 * t}$ Linear: $\frac{t}{q_{(t)}} = \frac{1}{k_2 * q_e^2} + \frac{t}{q_e}$	Pseudo second order kinetics	(5)
(S3)	Nonlinear: $q_e = \frac{q_{max} * k_L * [C_e]}{1 + k_L * [C_e]}$ Linear: $\frac{[C_e]}{q_e} = \frac{1}{k_L * q_{max}} + \frac{[C_e]}{q_{max}}$	Langmuir isotherm	(6)
(S4)	Nonlinear: $q_e = k_f * C_e^{\frac{1}{n}}$ Linear: $log\,(q_e) = log\,(k_f) + \frac{1}{n} * log(C_e)$	Freundlich isotherm	(6)
(S5)	$2 * d * sin\theta = n * \lambda$	Bragg's equation	(7)

Text S1. Calculation of effectiveness criterion. To determine the effectiveness criterion, parallel batch experiments were conducted with 46 mL solution of 10 mg L^{-1} of Hg^{2+}: (i) with 5.3 mg MoS_2@AC (as in typical adsorption experiment in this study) and (ii) with 1.7 mg MoS_2 nanosheets. The MoS_2 weight in both experiments was similar, as in supported form TGA suggested 30% MoS_2 coverage. The MoS_2 nanosheets were synthesized in the same method as described in the Methodology section for supported MoS_2.

The remaining mercuric concentration at equilibrium was found to be:

$$MoS_2: q_{Hg} = 126.9 \pm 8.7 \frac{mg}{g\ MoS_2}$$

$$MoS_2@AC:\ q_{Hg} = 200.2 \pm 4.5 \frac{mg}{g\ MoS_2}$$

Therefore, the effectiveness criterion was determined as:

$$Effectiveness\ criterion: \frac{NM@S}{NM} = \frac{200.2}{126.9} = 1.6$$

References

1. Cheng J, Li Y, Li L, Lu P, Wang Q, He C. Thiol-/thioether-functionalized porous organic polymers for simultaneous removal of mercury(II) ion and aromatic pollutants in water. New J Chem. 2019;43(20):7683–93.

2. Benjwal P, Kar KK. Simultaneous photocatalysis and adsorption based removal of inorganic and organic impurities from water by titania/activated carbon/carbonized epoxy nanocomposite. J Environ Chem Eng. 2015;3(3):2076–83.

3. Liu C, Wu P, Zhu Y, Tran L. Simultaneous adsorption of Cd(II) and BPA on amphoteric surfactant activated montmorillonite. Chemosphere. 2016;144:1026–32.

4. Jin X, Li Y, Yu C, Ma Y, Yang L, Hu H. Synthesis of novel inorganic–organic hybrid materials for simultaneous adsorption of metal ions and organic molecules in aqueous solution. J Hazard Mater. 2011;198:247–56.

5. Dong L, Li Q, Liao Q, Sun C, Li X, Zhao Q, et al. Characterization of molybdenum disulfide nanomaterial and its excellent sorption abilities for two heavy metals in aqueous media. Sep Sci Technol [Internet]. 2019;54(6):847–59. Available from: https://doi.org/10.1080/01496395.2018.1515226

6. Aghagoli MJ, Hossein Beyki M, Shemirani F. Application of dahlia-like molybdenum disulfide nanosheets for solid phase extraction of Co(II) in vegetable and water samples. Food Chem [Internet]. 2017;223:8–15. Available from: http://dx.doi.org/10.1016/j.foodchem.2016.12.023

7. Fausey CL, Zucker I, Lee DE, Shaulsky E, Zimmerman JB, Elimelech M. Tunable Molybdenum Disulfide-Enabled Fiber Mats for High-Efficiency Removal of Mercury from Water. ACS Appl Mater Interfaces. 2020;12(16):18446–56.